

REMOVAL OF REACTIVE BLUE 7 DYE FROM AQUEOUS SOLUTION USING SOLID WASTE

MOHAMED EL-SHAHATE ISMAIEL SARAYA & HASHAIM SAIED NASSAR

Department of Chemistry, Faculty of Science, Al-Azhar University, Nassr, Cairo, Egypt

ABSTRACT

Cement kiln dust (CKD) is a waste residue composed of oxidized generated as a by-product of the manufacture of Portland cement. In this study the CKD was used as an unconventional and low-cost adsorbent for the reactive blue 7 dye. The effect of adsorbent dose, contact time and initial dye concentration on removal efficiency of dye were investigated. Equilibrium adsorption isotherms and kinetics were studied. Besides, the dye-loaded CKD was investigated with XRD and FT-IR techniques. The results were shown the removal efficiency increases as CKD dose increase and contact time. The adsorption isotherm data were correspondent well to the Langmuir isotherm and the monolayer adsorption capacity was found to be 100 mg/g at 25 °C. This study showed that CKD has the potential to be used as a low-cost adsorbent. The investigations of dye-loaded CKD were shown the dye molecule reacted with soluble fraction on CKD dust to form insoluble salt.

KEYWORDS: Cement Kiln Dust, Reactive Blue 7, Isotherm; Kinetics, XRD, FTIR

INTRODUCTION

Wastewaters of textile and dyestuff industries are caused pollution of the environment and, therefore, they are toxic and carcinogenic, which causes serious hazards to aquatic living organisms [1, 2]. This is due to the fact that many of the dyes are made from hazardous materials that can cause many cancers, such as benzidine, naphthalene and other aromatic compounds [3]. Direct discharge of colored wastewater in the water bodies pollutes the aquatic environment by changing pH, chemical oxygen demand (COD), dissolved oxygen concentration, and biological oxygen demand (BOD) of water [4]. Therefore, dye removal from wastewater before disposal to the ecosystem such as the human diet is very important [5]. Various physical, chemical, and biological methods have been widely applied for the treatment of dye-containing wastewater [6-13]. Among the various categories of dyes, water-soluble reactive dyes are the most problematic because of the inability of conventional methods for their treatment and their high stability [14-17].

The complex aromatic nature of reactive dyes [18, 19], causes stability to heat, light, oxidizing agent and resistant to fading and biodegradability. So, effluent containing dyes are difficult removed using conventional biological and physicochemical processes [20, 21].

The Reactive Blue 7 is water soluble and is the most brilliant and is highly colored dyestuff [22]. It is used primarily in color for plastics, inks, metal surfaces, and dyestuffs for jeans and other clothing, pharmaceutical and computer industries [23]. The Reactive Blue 7 structure usually contains copper or nickel as the central metal ion. The wastewater lets out from the copper phthalocyanine dye has a high COD content and a significant amount of copper and

then leads to increase the heavy metal ions concentration in effluent. Reactive Blue 7 was decolorized using pellet-supported, Pd-catalyzed H₂ reduction [23], advanced oxidation processes [24], sonication [25], wet oxidative regeneration of powdered and granular activated carbon [26], and anaerobic granular sludge under mesophilic conditions [27].

Cement kiln dust (CKD) is a fine-grained caustic material that is generated as a solid waste of cement clinker manufacturing and its amount produced has been estimated around 15–20% of cement clinker production [28, 29]. It is composed of mixtures of calcined and uncalcined feed materials, some of sulfate, alkali, fuel combustion by-products and chloride compound [30]. There are many of environmental concerns related cement production especially emission and disposal of cement kiln dust [31]. CKD has high lime content, so it used as a neutralized of acidic wastewater [28, 32], for wastewater treatment [33], remove heavy metal ions from wastewater [34, 35], remove of acid dyes and direct dyes from aqueous solution [36, 37], as a stabilizing agent for soil [38], in a stabilization/solidification process [39, 40].

Therefore, the main objective of this study was to investigate the potential of cement kiln dust (CKD), an abundantly available solid waste, as an unconventional low-cost adsorbent in the removal of a dye Reactive Blue 7 from aqueous solutions. Also, rank the dye in dye loaded CKD.

MATERIALS AND METHODS

Materials

The materials that used in this investigation were Reactive Blue 7 (RB7) (Cibacron Turquoise Blue G, Cibacron Turquoise Blue G-E) purchased from Sigma –Aldrich and Cement kiln dust (CKD) was obtained from Torha cement Co located in the Helwan, Cairo, Egypt. The characteristics and chemical structures of RB7 are listed in Table 1. Some selected physico-chemical properties of the CKD are presented in Table 2. It can be seen that the CKD consists mainly of calcium oxide (CaO) and silica (SiO₂), with minor amounts of alumina (Al₂O₃) and iron oxide (Fe₂O₃), In addition to minor compounds such as, the sulfur trioxide (SO₃) and alkali (K₂O and Na₂O).

Table 1: Physico-Chemical Properties of Reactive Blue 7.

Chemical Name	Reactive Blue 7
Molecular formula	C ₄₁ H ₂₁ ClCuN ₁₄ Na ₄ O ₁₄ S ₅
Molecular Weight	1284.97
CAS Number	12238-09-4
C.I.	74460
λ max (nm)	619
Sulphonic group	4
Azo group	-
pH range	7.30
Chemical Structure	

Table 2: Physico-Chemical Properties of Cement Kiln Dust

Chemical Analysis*	Wt. %
SiO ₂	12.37
Al ₂ O ₃	3.36
Fe ₂ O ₃	1.36
CaO	34.6
MgO	1.81
SO ₃	3.22
K ₂ O	3.59
Na ₂ O	1.94
Cl	1.11
Free CaO***	21.73
LOI**	15.03
Total	100.52
Physical properties	
Retained on No. 325 sieve (%)	16.9
Average particle size	9.3 μm
Bulk density, g/ml	2.75
Specific surface area cm ² /g***	3180
pH	12.4
*Data obtained from the supplier	
**Loss on ignition at 1000 °C.	
***Blaine air permeability test	
***Chemical analysis	

Effect of Adsorbent Dose

The effect of CKD dose for the amount of RB7 adsorbed was studied by adding different amounts (0.2, 0.3, 0.4, 0.45, 0.50, 0.55, 0.6, 0.7, and 0.8 g) of CKD into a number of 250 ml Erlenmeyer flasks containing a definite volume (100 ml in each flask) of fixed initial concentration (600 mg/L) of dye solution without changing the solution pH at a temperature of 25 °C. The flasks were placed on a magnetic stirrer and stirring was provided at 120 rpm for 60 min.

Equilibrium Studies

The uptake experiments were carried out by adding a constant amount of sorbent (0.7 g) into a number of 250 ml Erlenmeyer flasks containing a definite volume (100 ml) of initial concentrations (200-600 mg/l) of dye solution without changing the solution pH at a temperature of 25 °C. The Erlenmeyer flasks were placed in a magnetic stirrer and stirring was provided at 120 rpm for 60 min to vouch equilibrium was reached. The concentrations of dye were measured at 619 nm wavelength, at time $t = 0$ and equilibrium. The adsorption at equilibrium, q_e (mg/g), was calculated by $q_e = ((C_o - C_e) V)/W$, and the dye removal can be calculated as, Removal efficiency % = $(C_o - C_e)/C_o$, where C_o and C_e (mg/l) are the concentrations of dye at initial and equilibrium, respectively, W (g) is the mass of dry adsorbent used and V (l) is the volume of the solution.

Effect of Solution pH

In this study 100 ml of dye solution of 600 mg/L initial concentration at different pH values (2.0–12.0) was stirred with 0.70 g of CKD in a water-bath shaker at 25 °C. Stirring was made for 60 min at a constant stirring speed of 120 rpm.

The pH was adjusted by 0.1N NaOH and 0.1N HCl solutions and measured using a pH meter (Hanna Instruments pH meters: HI 213 series).

Batch Kinetic Studies

The measures of kinetic experiments were mainly similar to those of equilibrium tests. The samples were taken at specified intervals of time to measured concentrations of dye. All the kinetic experiments were achieved without pH adjustment. The adsorption at time t , q_t (mg/g), was calculated as $q_t = ((C_0 - C_t) V)/W$, where C_t (mg/l) is the concentration of dye at time.

Analytical Measurements

The dye concentrations were measured by figuring out the absorbance characteristic wavelength using a double beam UV spectrophotometer (Shimadzu, Model UV 1800, Japan). A standard solution of the dye was prepared and the absorbance was determined at various wavelengths to obtain a plot of absorbance vs. wavelength. The wavelength corresponding to maximum absorbance (λ_{max}) was determined from this plot. The λ_{max} for RB7 was found to be 619 nm. Calibration curve was plotted between concentration of the dye solution and absorbance.

The colored residue was investigated using the Fourier transform infrared and x-ray diffraction. The spectroscopy (FT-IR) spectra of the products were recorded by Perkin Elmer 880 FT-IR spectrometer with the KBr pellet method. The XRD measurements were performed by diffractometer XRD 7000 (M/S. Shimadzu Instruments, Japan) with Ni filtered Cu $K\alpha$ as a radiation source at 2θ scan speed of 4° min^{-1} , $\lambda = 0.154 \text{ nm}$. The resulted XRD patterns were analyzed using X-Powder 12 software with the aid of ICDD PDF2 database.

RESULTS AND DISCUSSIONS

UV-Visible Spectra Studies

The changes in absorbance characteristics of RB7 dye during the removal process were investigated. The spectra showed that there was a maximum absorbance at 619 nm in the visible region. This peak is due to the blue color of the chromophore. The effect of adsorbent dose on the absorbance characteristics of RB7 are shown in Figure:1

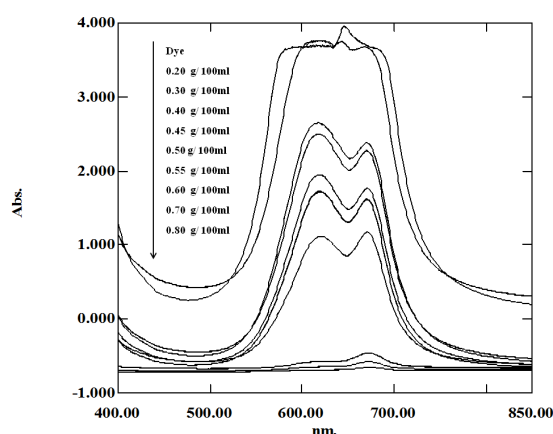


Figure 1: UV-Vis Absorption Spectrum of RB7 at Different Dose of CKD

The peak intensity decreases as the dose increases during the removal process. This may be because of the increasing of the alkalinity of solution ($\text{pH} > 12$) and soluble fraction of CKD with increasing the weight of CKD [31].

Zaki N. et al [41] were studied the effect of stirring time, temperature and initial weight of CKD on the percent CKD dissolved, they were reported that on washing CKD with water a portion of its weight is dissolved. The percentage dissolved is independent of stirring time and the original weight of CKD. Fig. 2 shows the changes of the UV/Vis spectra as function of time at different initial concentration of dye. All spectra show that the intensity of the absorbance peak at 619 nm, decreases with time which is attributable to the parent dye molecule, i.e. color, disappeared totally after about 25 to 10 min. for initial concentration from 500mg/l to 200 mg/l. When CKD dispersed in water the phases of CKD will either full dissolve or stable and partially soluble phases will precipitate. Thus the concentration of some constituent in CKD leachates will be controlled by the solubility of the intermediate phases, and the concentration of others will be controlled by their accessibility to the leachate solutions [42]. Duchesne and Reardon[43] were investigated the levels of pH and alkalinity of CKD leachates they found the alkalinity of CKD were established early during the reaction of CKD with water and do not change substantially with time, and pH values are very high ranging from about 13 to 13.6. Whereas dissolution of pure lime with water can be accounted for a maximum caustic alkalinity of about a pH of 12.4.

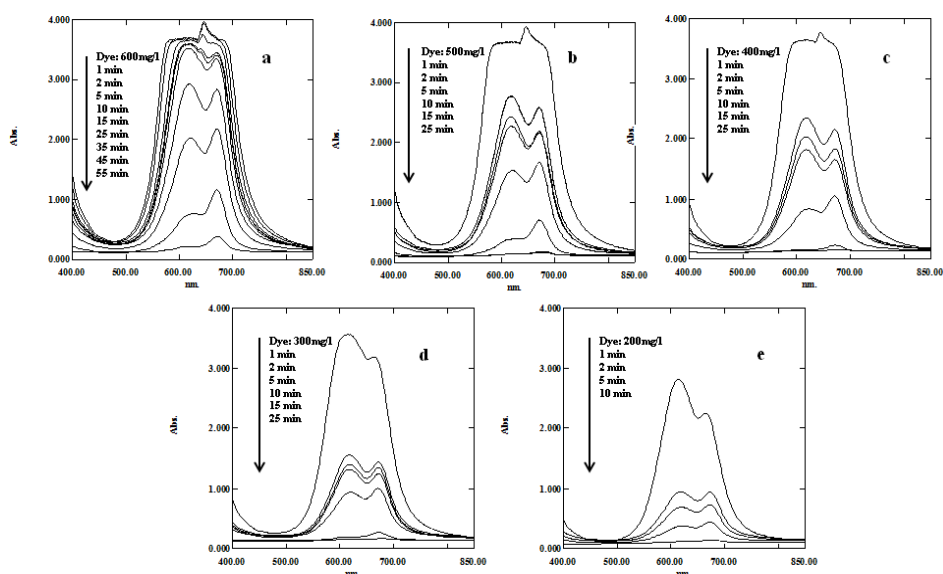


Figure 2: UV-Vis Absorption Spectrum of RB7 at Different Initial Concentration and Contact Time

The Effect of Operational Parameters on the Dye Removal Efficiency

Effect of adsorbent dose on dye removal

To investigate the effect of adsorbent dose (g) on dye removal, the experiments were conducted at initial dye concentration of 600 mg/L and shaken at 120 rpm. The relationship between the dye removal efficiency and the adsorbent dose is shown in Fig. 3 (a). It was observed that the dye removal efficiency increased from 50.15 % to 100.00% with increase in the adsorbent dose from 4 to 7 g/L. The increase in % color removal was due to the increase of the available sorption surface and availability of more adsorption sites, in addition to increase of the alkalinity [28]. Since no significant removal of Reactive Blue 7 was observed above 7g/L, it was selected as the optimum dosage.

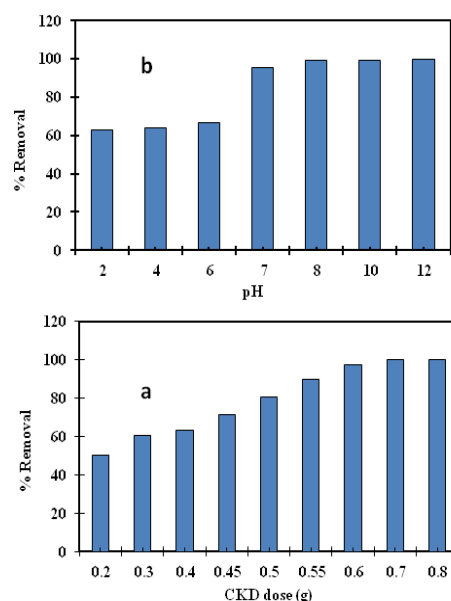


Figure 3: Effect of Adsorbent Dosage on the Adsorption of RB7 on CKD (A) And Effect of Solution Ph On the Adsorption of RB7 on 0.7 G Of CKD (B) at Temperature = 25 °C, $C_0 = 600$ Mg/L, Stirring Rate = 120 Rpm.

Effect of PH on Dye Removal

The relation between dye removal efficiency and initial pH of solution is shown in Fig. 3 (b). The results were shown that the RB7 dye removal was slightly changed over the pH value from 2 to 6, from 54.75 % to 57.3%. The dye removal efficiency was sharply increased when pH changed from acid media to basic, from 6 to 8, increased from 57.3 to 81.81. The dye adsorption was again time returned to become constant in alkaline media (from 8 to 12) with slightly increases of q_e (81.81 to 85.70 mg/g).

Effect of Initial Concentration and Contact Time on Dye Removal Efficiency

The effect of initial concentration on the adsorption of RB7 is shown in Fig. 4. It can be seen that the amount of RB7 removed per unit mass of adsorbent increased with the increase in initial concentration, although % removal percentage decreased with the increase in initial concentration. The amount of RB7 adsorbed at equilibrium (q_e) increased from 27.19 to 83.60 mg/g, as the initial concentration was increased from 200 to 600 mg/l. The initial concentration considered an impetus to overcome all mass transfer resistances of the RB7 between the aqueous and solid phases. Hence, a higher initial concentration of dye will improves the adsorption process. However, the RB7 % removal decreased from 100 % to 97.57%, as the RB7 concentration was increased from 200 to 600 mg/L.

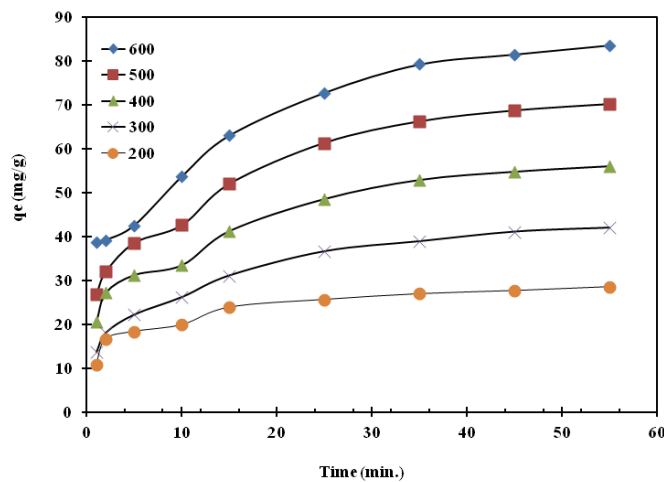


Figure 4: Effect of Contact Time and Initial Concentration on the Adsorption of RB7 on CKD (Temperature = 25 °C, W= 0.7 G/0.1l For RB7, C_o = 600 Mg/L, Stirring Rate = 120 Rpm).

Figure 4: Also shows the slow adsorption of RB7 in the first 10 min for all initial concentrations and then increases up to 35 min and thereafter, the adsorption rate decreases gradually until it reaches equilibrium. The equilibrium conditions were reached for RB7 within 25–30 min for initial concentrations less than 300 mg/l, 30–35 min for initial concentration less than 500 mg/l, while was needed 45 min for concentrations 600 mg/l.

Adsorption Isotherms

The Langmuir isotherm [44, 45] is represented by the following equation:

$$\frac{C_e}{q_e} = \frac{1}{q_m K_a} + \frac{C_e}{q_m} \quad (1)$$

Where q_e = the amount of adsorbate adsorbed per gram of the adsorbent at equilibrium (mg/g), C_e = the equilibrium concentration of adsorbate (mg/l⁻¹), q_m = maximum monolayer coverage capacity (mg/g), K_a = Langmuir isotherm constant (l/mg). The plots of C_e/q_e vs C_e are linear and illustrated in Figure. 5a. The values of q_m and K_a were computed from the slope and intercept of the Langmuir plot of Figure. 5a.

The equilibrium data were appropriated to Langmuir isotherm and the constants together with the R^2 value are listed in Table 3:

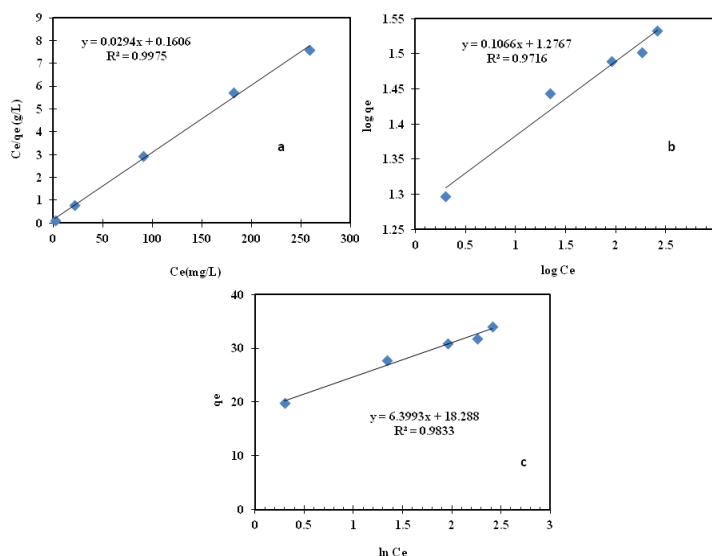


Figure 5: Adsorption Isotherms Curve of Adsorption of RB7 on CKD, Langmuir (A), Freundlich (B), Temkin (C)

Table 3: Isotherm Constants for Adsorption RB7 on CKD at 25 °c

Isotherm	Parameters
Langmuir	
qm (mg/g)	100
K_a (L/mg)	0.049
R^2	0.999
Freundlich	
K_F ((mg/g)(L/g) ^{1/n})	11.06
n	2.043
R^2	0.965
Temkin	
A (L/g)	2.38
B	23.21
R^2	0.997

The essential lineaments of the Langmuir isotherm may be expressed in terms of equilibrium parameter RL , which is a fixed dimensionless referred to as separation factor or equilibrium parameter that is given by Eq. (2) [46, 47].

$$RL = \frac{1}{(1 + K_a C_0)} \quad (2)$$

Where C_0 = initial concentration, K_a = the constant related to the energy of adsorption (Langmuir Constant).

The value of RL point to the shape of the isotherm to be either irreversible ($RL = 0$), linear ($RL = 1$), favorable ($0 < RL < 1$) or unfavorable ($RL > 1$) [48]. The adsorption becomes favorable when the RL values between 0 and 1. For adsorption of RB7 onto CKD, RL values obtained are shown in Fig. 6. The RL values for the adsorption of RB7 onto CKD are in the range from 0.0328 to 0.289, indicating that the adsorption is a favorable process and that at high initial concentration of RB7 the adsorption is nearly irreversible. From this, the maximum monolayer coverage capacity (qm) from Langmuir Isotherm model was determined to be 100 mg/g, K_a (Langmuir isotherm constant) is 0.049 L/mg and the R^2 value is 0.999 for RB7 proving that the sorption data fitted well to Langmuir Isotherm model.

The logarithmic form of the Freundlich isotherm equation is given as

$$\log q_e + \frac{1}{n} \log C_e \quad (3)$$

Where q_e = the amount of dye adsorbed per gram of the adsorbent (mg/g), C_e = the equilibrium concentration of adsorbate (mg/L), K_f = Freundlich isotherm constant (mg/g), n = adsorption intensity. Freundlich constants can be calculated from the slope and intercept of plot in Fig. 5b, and are given in Table 3.

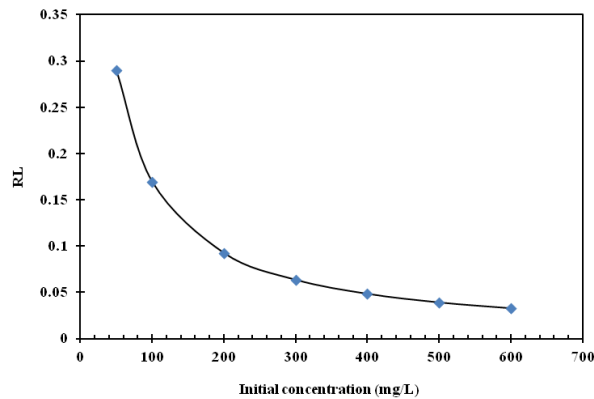


Figure 6: The Separation Factor for RB7 Adsorption on CKD at 25 °C

The constant K_f is a function of adsorption capacity, while $1/n$ is an indicator of the strength of adsorption [49, 50]. If $n = 1$ then the partition between the two phases is independent of the concentration. If a value of $1/n$ is less than one, it indicates a normal adsorption. On the other hand, $1/n$ being above one indicates cooperative adsorption [51]. As seen in Table 3, it was found that the Freundlich model yields a less better, $R^2 = 0.965$ compared with that of the Langmuir model ($R^2 = 0.999$ for RB7). In addition, the values of $1/n$ is 0.4779 for RB7 while $n = 2.043$ for RB7, which suggested that the adsorption of RB7 on CKD were favorable.

The model of Temkin Isotherm [52, 53] is given by the following equation

$$q_e = B \ln A_T + B \ln C_e \quad (4)$$

$$\text{where } B = \frac{RT}{b} \quad (5)$$

Where A_T = Temkin isotherm equilibrium binding constant (L/g), b_T = Temkin isotherm constant, R = universal gas constant (8.314 J/mol/K), T = Temperature at 298K, B = Constant related to heat of sorption (J/mol). By plotting the q_e against $\ln C_e$ and the constants were determined from the slope and intercept of Fig. 5c.

The constants A and B together with the R^2 values are shown in Table 3. From the Temkin plot shown in Fig. 5c, the following values were evaluated: $A_T = 2.38$ L/g, $B = 23.21$ J/mol which is function of the heat of sorption indicating a physical adsorption process and the $R^2 = 0.997$.

Adsorption Kinetics

The rate constants for the adsorption of RB 7 on CKD were determined using pseudo-first-order, pseudo-second-order equations and intraparticle diffusion. The pseudo-first-order model was described [54] as

$$\log(q_e - q_t) = \log q_e - \frac{k_1 t}{2.303} \quad (6)$$

Where k_1 is the rate constant of pseudo-first-order adsorption, q_e and q_t are the amounts of adsorption at equilibrium and at time t , respectively and presented in (Fig. 7a). If the plot was found to be linear with good correlation coefficient, it indicates that equation is appropriate to RB7 sorption on CKD. So, the adsorption process is a pseudo-first-order process [51, 54]. It was observed that the pseudo-first-order model did not fit well. It was found that the calculated q_e values did not agree with the experimental q_e values, Table 4. This suggests that the adsorption of RB7 did not follow first-order kinetics. The pseudo-second-order kinetics may be expressed as [49, 54, 55]:

$$\frac{t}{q_t} = \frac{1}{k_2 q_e^2} + \frac{t}{q_e} \quad (7)$$

Where k_2 is the rate constant for pseudo-second-order adsorption. The k and q_e can be directly gained from slope and the intercept of the plot of t/q_t vs t and presented in Fig. 7b. It can be seen from Table 4 that the adsorption kinetics can be represented by the pseudo-second-order model, suggesting that the adsorption process was guided by chemisorption [56]. The initial adsorption rates h (mg/g min) can be counted from the pseudo-second-order model by the following equation

$$h_{0,2} = k_2 q_e^2 \quad (8)$$

Table 4: Comparison of The Pseudo-First-Order, Pseudo-Second-Order Adsorption Rate Constants and Calculated and Experimental Q_e Values Obtained At Different Initial RB7 Concentrations

Initial Concentration	$Q_{e,Exp}$ (Mg/G)	Pseudo-First Order Kinetic Model			Pseudo-Second Order Kinetic Model			
		K_1 (1/min)	$q_{e,cal}$ (mg/g)	R^2	K_2 (1/min)	$q_{e, cal}$ (mg/g)	R^2	h_0
200	28.57	0.06448	15.00	0.9844	0.010929	29.76190	0.9965	9.68054
300	41.96	0.07270	30.63	0.9843	0.004392	45.45455	0.9962	9.07441
400	55.98	0.07323	39.37	0.9863	0.003585	59.88024	0.9957	12.85347
500	70.14	0.07484	49.90	0.9889	0.002953	74.62687	0.9968	16.44737
600	83.63	0.07140	55.70	0.9922	0.002529	89.28571	0.9986	20.16129

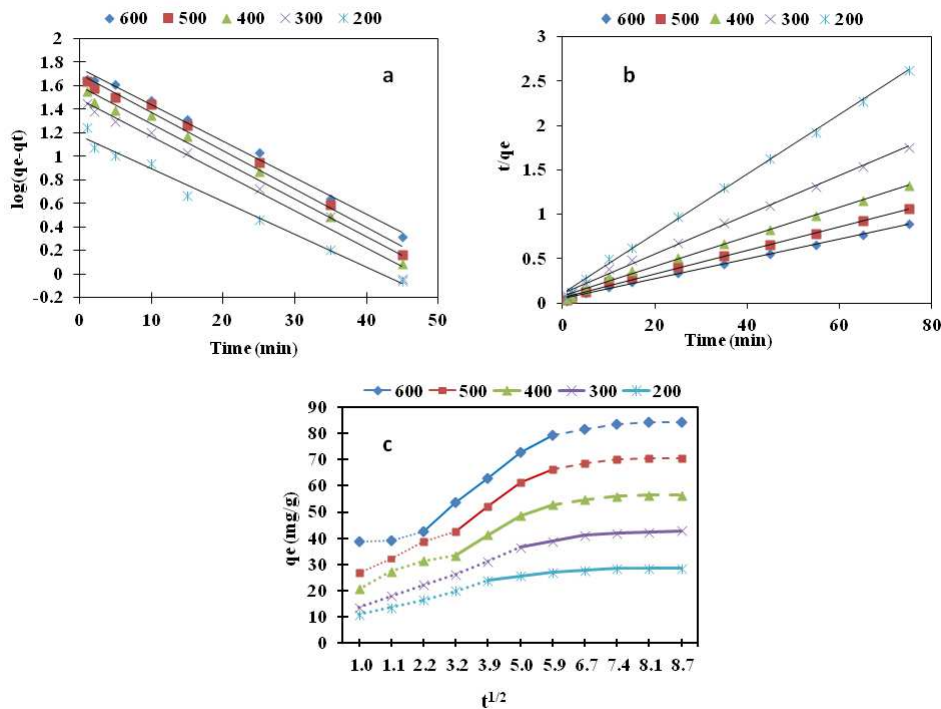


Figure 7: Pseudo-First Order (A) Pseudo-Second Order (B) and Intraparticle Diffusion (C) Plots For Removal of RB7dye on CKD with Different Initial Concentrations At 25 °C

It was found that the initial rate of adsorption increases with increasing initial concentration of RB7, which would be expected due to the increase in driving force at higher concentration.

The possibility of intraparticle diffusion was explored by using an intraparticle diffusion model [57]. It is an empirically get functional relation, common to the most adsorption processes, where removal change almost proportionally with $t^{1/2}$ rather than with the contact time t . According to this theory:

$$q_t = k_{id}t^{1/2} + C_i \tag{9}$$

Where k_{id} ($mg/g \text{ min}^{1/2}$), the rate parameter of stage i , is determined from the slope of the straight line of q_t vs $t^{1/2}$, (Fig. 7c). C_i , the intercept of stage i , illustrate the thickness of the boundary layer, i.e., the larger the intercept, the greater the boundary layer effect. If intraparticle diffusion takes place, then q_t versus $t^{1/2}$ will be linear and if the plot runs through the origin, then the rate constraining process is only due to the intraparticle diffusion [58]. For intraparticle diffusion plots, the first, sharper region is the spontaneous adsorption or external surface adsorption. The second region is the progressive adsorption stage where intraparticle diffusion is the rate limiting. In some cases, the third region presents, which is the final equilibrium stage where intraparticle diffusion beginning to delayed down due to the very low adsorbate concentrations left in the solutions [58]. Referring to Fig. 7c, for all initial concentrations, the first stage was carried out within the first 25 min and the second stage of intraparticle diffusion control was then attained. The third stage only occurred for higher RB7 initial concentration of 200, 300, 400, 500 and 600 mg/l. The different stages of rates of adsorption observed assigned to that the adsorption rate were initially faster and then decelerated when the time increased. As seen from Fig. 7b, the plots were not linear over the whole time range, this means that the adsorption process are affected by more than one process.

Kinetic parameters for their three kinetics models and correlation coefficients are summarized in Table 5.

Table 5: Intraparticle Diffusion Model Constants and Correlation Coefficients for Adsorption of Rb7 on Ckd at 25 °c

Initial Concentration	K_{p1} (Mg/G Min ^{1/2})	C_1	$(R_1)^2$	K_{p2} (Mg/G Min ^{1/2})	C_2	$(R_2)^2$	K_{p3} (Mg/G Min ^{1/2})	C_3	$(R_3)^2$
200	3.6913	8.2564	0.9401	1.0050	20.583	0.9228	-	-	-
300	5.3228	10.094	0.9592	1.6993	28.770	0.9295	-	-	-
400	4.9198	18.932	0.7817	4.8190	23.466	0.9062	0.4345	52.848	0.7713
500	6.5760	22.663	0.9210	5.9170	30.270	0.9628	0.2276	68.500	0.7713
600	3.1115	35.579	0.9993	9.1421	26.178	0.9845	2.061	67.931	0.9330

Removal Mechanism

The adsorbent dye, RB7, on cement kiln dust was tracked by analysis of dye loaded cement kiln dust. The interaction of CKD with a given reactive blue7 dye depends on the chemical and physical characteristics of the CKD. The reactivity of the oxides in the CKD is significantly different that may be it has different mineralogical structure. The major mineral phases present in CKD were calcium carbonate (calcite), free-lime (CaO) and quartz (SiO₂) as are shown from Fig. 8. Besides of arcanite (K₂SO₄) and sylvite (KCl) were identified. Fig. 8 shows the X-ray diffraction pattern obtained for the washed CKD. The dominating calcite peaks and the quartz peaks present in CKD powder remained unchanged in the washed CKDs, indicating the inert nature of these two compounds. It also appears that all free-lime content in the CKDs was converted to calcium hydroxide (CH). The crystalline alkali sulfates phases, such as arcanites (K₂SO₄) and sylvite (KCl), present in dry CKDs were not retained in the washed CKD products, indicating the high solubility of these materials [35, 41]. When dye solution treated with CKD there are some changes occurred in the intensity of characteristics peaks of calcium hydroxide that related to interaction between dye molecules, i.e. sulfonate and amino function groups, and Ca⁺⁺. Fig. 9 Shows the FT-IR spectra of washed CKD and dye-loaded CKD. The FTIR spectrum of CKD is shown in Fig. 9, the peaks positions at 1448, 868.7 and 715 cm⁻¹ are related to calcite that is considered as the main phase in CKD. The band at 3640-3693 cm⁻¹ is due to OH⁻ and 3427 cm⁻¹ is due to H₂O, while the bands at 1025.9 cm⁻¹ correspond to silicate, Si-O groups, respectively[59, 60].

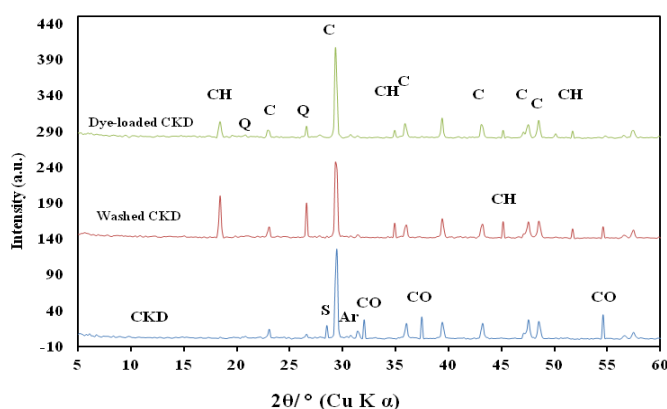


Figure 8: X-Ray Patterns of Ckd, Washed Ckd and Dye-Loaded Ckd (Ch–Calcium Hydroxide, Q–Quartz, C–Calcite, S–Sylvite, Ar–Arcanite, Co–Free-Lime (Calcium Oxide))

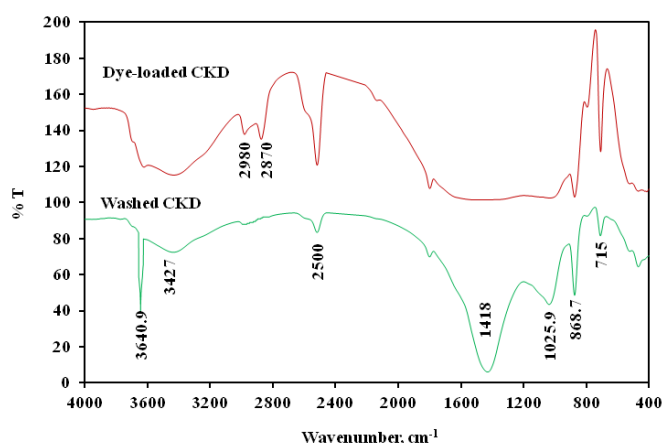


Figure 9: FTIR Spectra of Washed CKD and Dye-Loaded CKD

FTIR spectra of dye loaded-CKD are shown in Fig. 9. The characteristic bands of calcite still presence with some change on it intensity that may related to adsorption of dye molecules, that conformed by appear new bands at 2980 and 2870 cm^{-1} due to symmetric and asymmetric CH_2 stretching of dye. On the other hand the intensity of characteristic band of hydroxide radical, at 3640 cm^{-1} , is sharply decreased that can be attributed to dissolution of calcium hydroxide and interacted with function groups of dye molecule, such as $-\text{SO}_3^-$. Also broad peak from 1100-1700 cm^{-1} include many characteristic peaks for different groups such as symmetric and asymmetric $-\text{COO}-$ stretching of carboxylate bond at 1587 cm^{-1} , $-\text{SO}_3^-$ group at 1238 cm^{-1} . This indicates

To follow the dye, the dye loaded CKD was treated with different liquids such as water, methanol, ethanol, nitric acid and hydrochloric acid. About 1 g of dye loaded CKD was stirred with 100 ml of each liquid and then filtered; Fig. 10 is shown the UV-vis spectra of filtrates. The UV vis spectra of the samples that washed with water, methanol and ethanol are shown a very slightly appearance to characteristic peak of RB7 dye at 619 nm. On the other hand the samples that were treated with nitric and hydrochloric acid do not shown any band for RB7. Although it shows new band that may be related to the degradation of dye or change the structure of dye molecule through change the chromophore groups.

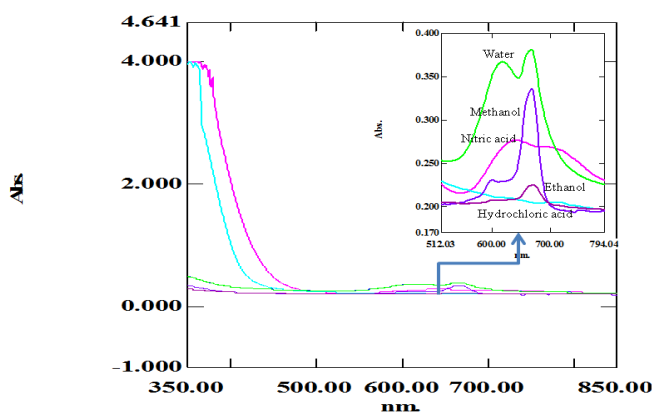


Figure 10: UV-Vis Absorption Spectrum of Filtrates of Dye-Loaded CKD After Treated with Different Solvent and Acids

We speculated that there are chemical interaction between function groups of dye molecule and CKD constituents [4, 14, 60] as the following:



Figure 11: is shown the Effect of thermal treatment on the colored cement kiln dust. It is shown that the color of residue disappears after thermal treatment up to 650 °C and the color of cement kiln dust returned to its original color. This is mainly due to decomposition of dye into carbon dioxide and water.



Figure 11: Effect of Thermal Treatment on Dye-Loaded CKD

CONCLUSIONS

The effect of various operational parameters such as contact time, CKD dust amount and initial dye concentration on the adsorption of Reactive Blue 7 dye was investigated and optimized. The CKD used as a low-cost adsorbent showed an excellent adsorption performance for removal of RB7 dye from aqueous solutions. The maximum adsorption capacity of CKD was found to be 100 mg/g of CKD at 25 °C. The kinetics of the adsorption process was found to rank the pseudo-second-order kinetic model, which indicates that the adsorption process was guided by chemisorption. The plots of intraparticle diffusion model were not linear over the all of the time range, which means that more than one process touched the adsorption. The XRD and FTIR analysis were shown the concentration of some CKD constituents are reduced that may be attributed to its reaction with dye molecules. The treatment of dye-loaded CKD with different solvent and acids were shown that very slightly amount of dye released in water, methanol and ethanol that may be a result of physically adhesion dye. While in case of acid the dye-loaded CKD was dissolved and change. This is mainly due to interaction of dye molecule with CKD. The cement kiln dust used in this work is freely and abundantly available, do not require an additional pretreatment process such as activation before applications and possess high adsorption capacity for RB7. Therefore, the adsorbent is expected to be economically feasible for removal of RB7 dye from aqueous solutions.

REFERENCES

1. Y. Wong, Y. Szeto, W. Cheung, G. McKay, Adsorption of acid dyes on chitosan equilibrium isotherm analyses. *Process Biochem.*, (2004) 39: 695-704.
2. M. Safarikova, L. Ptáčková, I. Kibrikova, I. Šafařík, Biosorption of water-soluble dyes on magnetically modified *Saccharomyces cerevisiae* subsp. *uvarum* cells. *Chemosphere*, (2005) 59:831-835.

3. G. Kyzas, N. Lazaridis, Reactive and basic dyes removal by sorption onto chitosan derivatives. *J. Colloid. Interface Sci.*, (2009) 331:32-39.
4. P. Bedekar, R. Saratale, G. Saratale, S. Govindwar, Oxidative stress response in dye degrading bacterium *Lysinibacillus* sp. RGS exposed to reactive orange 16, degradation of RO16 and evaluation of toxicity. *Enviro. Sci. Pollut. R.*, (2014) 21:11075-11085.
5. K. Kumar, K. Porkodi, Mass transfer, kinetics and equilibrium studies for the biosorption of methylene blue using *Paspalum notatum*. *J. hazardous mater.*, (2007) 146:214-226.
6. I. Kiran, T. Akar, A. Ozcan, A.S. Ozcan, S. Tunali, Biosorption kinetics and isotherm studies of acid red 57 by dried *Cephalosporium aphidicola* cells from aqueous solutions. *Biochem. Eng. J.*, (2006) 31:197-203.
7. L. Lackey, R. Mines, P. Mc Creanor, Ozonation of acid yellow 17 dye in a semi-batch bubble column. *J. Hazardous Mater. B.*, (2006) 138:357-362.
8. A. Koparal, Y. Yavuz, C. Gurel, U. Ogutveren, Electrochemical degradation and toxicity reduction of C.I. basic red 29 solution and textile wastewater by using diamond anode. *J. Hazardous Mater.*, (2007) 145:100-108.
9. M. Panizza, G. Cerisola, Direct and mediated anodic oxidation of organic pollutants, *Chemical Rev.*, (2009) 109:6541-6569.
10. M. Dehghani, A. Najafpoor, K. Azam, Using sonochemical reactor for degradation of LAS from effluent of wastewater treatment plant, *Desalination*, (2010) 250:82-86.
11. D. Gumus, F. Akbal, Photocatalytic degradation of textile dye and wastewater, *Water Air Soil Poll.*, (2011) 216:117-124.
12. H. Akdogan, M. Canpolat, Removal of reactive orange 16 by immobilized *Coprinus plicatilis* in the batch shaking bioreactor, *Fiber Polym.*, (2013) 14:76-81.
13. I. Grčić, S. Papić, K. Žižek, N. Koprivanac, Zero-valent iron (ZVI) Fenton oxidation of reactive dye wastewater under UV-C and solar irradiation, *Biochem. Eng. J.*, (2012) 195:77-90.
14. K. Rajkumar, M. Muthukumar, Optimization of electro-oxidation process for the treatment of reactive orange 107 using response surface methodology, *Environ. Sci. Pollut. R.*, (2012) 19:148-160.
15. Ch-H Wu, Effects of operational parameters on the decolorization of C.I. Reactive Red 198 in UV/TiO₂ based systems, *Dyes Pigments*, (2008) 77:31-38.
16. M. Muthukumar, M. Karupiah, G. Raju, Electrochemical removal of CI acid orange 10 from aqueous solutions, *Sep. Purif. Technol.*, (2007) 55:198-205.
17. N. Supaka, K. Juntongjin, S. Damronglerd, M. Delia, P. Strehaiano Microbial, decolonization of reactive azo dyes in a sequential anaerobic-aerobic system, *Chem. Eng. J.*, (2004) 99:169-176.
18. C. Tang, V. Chen, The photocatalytic degradation of reactive black 5 using TiO₂/UV in an annular photoreactor,

- Water Res., (2004) 38:2775–2781.
19. D. Ju, I. Byun, J. Park, C. Lee, G. Ahn, T. Park, Biosorption of a reactive dye (Rhodamine-B) from an aqueous solution using dried biomass of activated sludge, *Bioresource Technol.*, (2008) 99:7971-7975.
 20. S. Mondal, Methods of dye removal from dye house effluent: an overview, *Environ. Eng. Sci.*, (2008) 25:383–396.
 21. G. Gadd, Biosorption: critical review of scientific rationale, environmental importance and significance for pollution treatment, *J. Chem. Technol. Biot.*, (2009) 84:13–28.
 22. A.C. Basha, R. Saravanathamizhan, V. Nandakumar, K. Chitra, C. Lee, Copper recovery and simultaneous COD removal from copper phthalocyanine dye effluent using bipolar disc reactor., *Chem. Eng. Res. Des.*, (2013) 91:552-559.
 23. R. Matthews, L. Bottomley, S. Pavlostathis Palladium-catalyzed hydrogen reduction and decolorization of reactive phthalocyanine dyes, *Desalination*, (2009) 248:816-825.
 24. I. Grčić, S. Papić, N. Koprivanac, I. Kovačić, Kinetic modeling and synergy quantification in sono and photooxidative treatment of simulated dye house effluent, *Water Res.*, (2012) 46:5683-5695.
 25. E. Fontenot, Y. Lee, R. Matthews, G. Zhu, S., Pavlostathis Reductive decolorization of a textile reactive dye bath under methanogenic conditions, *Appl. Biochem. Biotech.*, (2003) 109:207-225.
 26. R. Shende, V. Mahajani, Wet oxidative regeneration of activated carbon loaded with reactive dye, *Waste Manage.*, (2002) 22:73-83.
 27. 2A. Dos Santos, F. Cervantes, J. Van Lier, Review paper on current technologies for decolourisation of textile wastewaters: perspectives for anaerobic biotechnology. *Bioresource Technol.*. (2007) 98:2369-2385.
 28. A. Mackie, M. Walsh., Bench-scale study of active mine water treatment using cement kiln dust (CKD) as a neutralization agent, *Water Res.*, (2012) 46:327-334.
 29. Mackie, S. Boilard, M. Walsh, C. Lake, Physicochemical characterization of cement kiln dust for potential reuse in acidic wastewater treatment, *J. Hazard. Mater.*, (2010) 173:283–291.
 30. R. Siddique, A. Rajor, Influence of bacterial treated cement kiln dust on the properties of concrete. *Constr. Build. Mater.*, (2014) 52 42-51.
 31. N. Zaki, I. Khattab, N. Abd El-Monem, Removal of some heavy metals by CKD leachate, *J. Hazard. Mater.* (2007) 147:21-27.
 32. A. Mohamed, M. El Gamal, Solidification of cement kiln dust using sulfur binder, *J. Hazard. Mater.*, (2011) 192:576– 584.
 33. Ahmad, R. Ghufuran, Z. Abdel Wahid, Role of calcium oxide in sludge granulation and methanogenesis for the treatment of palm oil mill effluent using UASB reactor, *J. Hazard. Mater.*, (2011) 198:40– 48.
 34. O. Ali, H. Osman, S. Sayed, M. Shalabi, The removal of some rare earth elements from their aqueous solutions on

- by-pass cement dust (BCD), *J. Hazard. Mater.*, (2011) 195:62–6.
35. A. Salem, H. Afshin, H. Behsaz, Removal of lead by using Raschig rings manufactured with mixture of cement kiln dust, zeolite and bentonite, *J. Hazard. Mater.*, (2012) 223:13-23.
 36. E. Mahmoud, Cement kiln dust and coal filters treatment of textile industrial effluents, *Desalination*, (2010) 255:175 –178.
 37. M. Saraya, M. Aboul-Fetouh, Utilization from cement kiln dust in removal of acid dyes, *Am J of Environ Sci.*, (2012) 8:16-24.
 38. O. Peyronnard, M. Benzaazoua, Alternative by-product based binders for cemented mine backfill: Recipes optimisation using Taguchi method, *Miner. Eng.*, (2012) 29:28–38.
 39. K. Carlson, F. Sariosseiri, B. Muhunthan, Engineering properties of cement kiln dust modified soils in western washington state, *Geotechn. Geol. Eng.*, (2011) 29:837-844.
 40. A. Ebrahimi, T. Edil, Y. Son, Effectiveness of cement kiln dust in stabilizing recycled base materials, *J. Mater. Civil Eng.*, (2011) 24:1059-1066.
 41. S. Peethamparan, J. Olek, J. Lovell, Influence of chemical and physical characteristics of cement kiln dusts (CKDs) on their hydration behavior and potential suitability for soil stabilization, *Cement Concrete Res.*, (2008) 38:803-815.
 42. L.E. Eary, D. Rai, S.V. Mattigod, C.C. Ainsworth Geochemical factors controlling the mobilization of inorganic constituents from fossil fuel combustion residues: II. Review of the minor elements, *J. Environ. Qual.*, (1990) 19:202-214.
 43. J. Duchesne, E.J. Reardon Determining controls on element concentrations in cement kiln dust leachate, *Waste Manage.*, (1998) 18: 339-350.
 44. G. Alberti, V. Amendola, M. Pesavento, R. Biesuz, Beyond the synthesis of novel solid phases: review on modelling of sorption phenomena, *Coordin. Chem. Rev.*, (2012) 256:28-45.
 45. M. Ghaedi, J. Tashkhourian, A. Pebdani, B. Sadeghian, F. Ana, Equilibrium, kinetic and thermodynamic study of removal of reactive orange 12 on platinum nanoparticle loaded on activated carbon as novel adsorbent, *Korean J. Chem. Eng.*, (2011) 28:2255-2261.
 46. K. Hall, L. Eagleton, A. Acrivos, T. Vermeulen, Pore-and solid-diffusion kinetics in fixed-bed adsorption under constant-pattern conditions, *Ind. Eng. Chem. Fund.*, (1966) 5:212-223.
 47. T. Weber, R. Chakravorti, Pore and solid diffusion models for fixed-bed adsorbers, *AIChE J.*, (1974) 20:228-238.
 48. Hameed, Spent tea leaves: a new non-conventional and low-cost adsorbent for removal of basic dye from aqueous solutions, *J. Hazard. Mater.*, (2009) 161:753-759.
 49. Z. Komy A. Shaker, S. Heggy, M. El-Saye, Kinetic study for copper adsorption onto soil minerals in the absence

- and presence of humic acid, *Chemosphere*, (2014) 99:117-124.
50. M. Moazeni, H. Hajipour, M. Askari, M. Nusheh, Hydrothermal synthesis and characterization of titanium dioxide nanotubes as novel lithium adsorbents, *Mater Res Bull.*, (2015) 61:70-75.
 51. Y. Ho, G. McKay, Sorption of dye from aqueous solution by peat, *Cheml. Eng. J.*, (1998) 70:115–124.
 52. [52] C. Aharoni, M. Ungarish, Kinetics of activated chemisorption, Part 2. Theoretical models, *Journal Chemical Society, Faraday Trans.*, (1977) 73:456–464.
 53. Y. Foo, B. Hameed, Insights into the modeling of adsorption isotherm systems, *Chem. Eng. J.*, (2010) 156: 2-10.
 54. Hameed, D. Mahmoud, A. Ahmad, Equilibrium modeling and kinetic studies on the adsorption of basic dye by a low-cost adsorbent: Coconut (*Cocos nucifera*) bunch waste, *J. Hazard. Mater.*, (2008) 158:65-72.
 55. Y. Ho, G. McKay, The kinetics of sorption of divalent metal ions onto sphagnum moss peat, *Water Res.*, (2000) 34:735–742.
 56. W. Tsai, H. Hsu, T. Su, K. Lin, C. Lin, T. Dai, The adsorption of cationic dye from aqueous solution onto acid-activated andesite, *J. Hazard. Mater.*, (2007) 147:1056–1062.
 57. N. Amin, Removal of reactive dye from aqueous solutions by adsorption onto activated carbons prepared from sugarcane bagasse pith, *Desalination*, (2008) 223:152-161.
 58. W. Cheung, Y. Szeto, G. McKay, Intraparticle diffusion processes during acid dye adsorption onto chitosan, *Bioresource Technol.*, (2007) 98: 2897–2904.
 59. J. Asaad, S. Tawfik, Polymeric composites based on polystyrene and cement dust wastes, *Mater. Design*, (2011) 32:5113-5119.
 60. Kaušpēdienė, A. Gefenienė, E. Kazlauskienė, R. Ragauskas, A. Selskienė, Simultaneous removal of azo and phthalocyanine dyes from aqueous solutions using weak base anion exchange resin, *Water Air Soil Poll.*, (2013) 224:1-12.